CORA Cork Open Research Archive
Cartlann Taighde Oscailte Chorcaí

Title	Calculations of the A(1) phonon frequency in photoexcited tellurium
Authors	Tangney, P;Fahy, Stephen B.
Publication date	1999
Original Citation	Tangney, P. and Fahy, S. (1999) ' Calculations of the A(1) phonon frequency in photoexcited tellurium', Physical Review Letters, 82(21), 4340-4343 (4pp). doi: 10.1103/PhysRevLett.82.4340
Type of publication	Article (peer-reviewed)
Link to publisher's version	https://journals.aps.org/prl/abstract/10.1103/PhysRevLett.82.4340 - 10.1103/PhysRevLett.82.4340
Rights	© 1999, American Physical Society
Download date	2026-11-01 13:18:24
Item downloaded from	https://hdl.handle.net/10468/4660

UCC
University College Cork, Ireland
Coláiste na hOllscoile Corcaigh

Calculations of the A_1 Phonon Frequency in Photoexcited Tellurium

P. Tangney and S. Fahy
Department of Physics, University College, Cork, Ireland
(Received 19 October 1998)

Calculations of the A_1 phonon frequency in photoexcited tellurium are presented. The phonon frequency as a function of photoexcited carrier density and phonon amplitude is determined. Recent pump-probe experiments are interpreted in light of these calculations. It is proposed that, in conjunction with measurements of the phonon period in ultrafast pump-probe reflectivity experiments, the calculated frequency shifts can be used to infer the evolution of the density of photoexcited carriers on a subpicosecond time scale. [S0031-9007(99)09219-4]

PACS numbers: 78.47.+p, 63.20.Kr, 63.20.Ry

During the past decade, continuing advances in ultrafast laser technology have made possible time-domain studies of coherent phonons on ever shorter time scales [1,2]. In pump-probe experiments it has been possible to excite a high density of electrons in a semiconductor on a time scale much smaller than the lattice vibrational period and detect the resulting motion of the ions by observing oscillations in the optical reflectivity [3]. In certain materials, femtosecond laser pulses may be used to excite electrons from bonding into antibonding states, thereby depleting the bond charge and changing the equilibrium positions of the atoms; the atoms then oscillate about their new equilibrium—a mechanism known as "displacive excitation of coherent phonons" (DECP) [4]. At very high excitation densities, the bonds may be weakened and the resulting motion has a frequency lower than that observed in conventional Raman scattering. In recent femtosecond pump-probe experiments, Hunsche *et al.* [3] reported a linear decrease of the tellurium A_1 phonon frequency and an increase of the phonon amplitude with pump fluence. Moreover, they observed that at high excitation densities the periods of successive single cycles of the oscillations after the pump excitation tended to decrease.

In this Letter, we calculate from first principles the dependence of the Te A_1 phonon frequency on the density of excited electrons, thus opening the possibility of using the measured shift in phonon frequency to probe local electron-hole plasma density on a subpicosecond time scale. We calculate the dependence of frequency and equilibrium bond length on excitation density. We also calculate the initial phonon amplitude as a function of excited electron density, within the DECP mechanism. Finally, we calculate the amplitude dependence of the phonon frequencies and predict a significant anharmonicity of the A_1 phonon at very high carrier densities.

If a laser pulse of duration much shorter than the time scale of the ionic motion is incident on a crystal, then an effectively instantaneous photoexcited carrier distribution is created. Initially, the electron and hole distributions will be nonthermal, but carrier-carrier scattering [5] will result in a thermal (Fermi-Dirac) distribution of electrons and of the holes in much less than 100 fs, the time scale of phonon motion.

At the high electron-hole densities excited in the pump-probe experiments, one may expect a considerable enhancement of the usual electron-hole recombination rate (of the order of 1 ns [1]) found in semiconductors [6]. However, since the double-pulse excitation experiments of Hunsche *et al.* [3] show no substantial change in the A_1 phonon lifetime as the electron-hole density is altered (see Fig. 5 of Ref. [3]), the rate for electron-hole recombination cannot be of the same order as the phonon period. (A relaxation channel with the same time scale as the period of a mode leads to strong dissipation of that mode [7].) Thus, electron-hole recombination occurs on a time scale either substantially longer or substantially shorter than the A_1 phonon period. We will consider both alternatives, although the latter is unlikely since estimates [6] suggest a maximum rate of the order of 1 ps for electron-hole recombination in materials at high electronic excitation.

Although some of the carrier energy will be lost to the lattice by carrier-optical-phonon scattering, and this may lead to heating of the lattice on the time scale of several A_1 phonon periods, this will not affect the electron-hole density. The double-pulse excitation experiments of Hunsche *et al.* [3] suggest that the effect of such lattice heating on the A_1 phonon frequency is small.

In comparing with the experimental measurements [3], the effects of carrier diffusion must be taken into consideration. Assuming [3] an ambipolar diffusion rate in the excited material equal to that for low plasma density ($D = 40\ \mathrm{cm}^2/\mathrm{s}$) and an absorption length of $l = 50$ nm for the pump optical pulse (wavelength 825 nm), the electron-hole density at the surface falls to 0.43 of its initial value in a time $l^2/D = 0.6$ ps (approximately twice the period of the A_1 phonon), to 0.34 in 1.2 ps, and to 0.26 in 2.4 ps. Thus, the phonon period measured by the surface reflectivity is constantly changing due to the diffusion of carriers away from the surface [3].

With these physical time scales in mind, in most of the present calculations we assume that no electron-hole recombination occurs during phonon oscillations. There

 0031-9007/99/82(21)/4340(4)$15.00 © 1999 The American Physical Society

will then be a constant density of electrons in the conduction bands, with an equal density of holes in the valence bands (treating carrier diffusion at a later stage of the analysis). A Fermi-Dirac distribution of each carrier type is assumed, but the chemical potential for electrons μ_{e^-} and for holes μ_{h^+} are not equal. Previous theoretical investigations [8–10] of short-time phonon dynamics in semiconductors subjected to electronic excitation by ultrashort laser pulses have assumed that the chemical potential for electrons μ_{e^-} and for holes μ_{h^+} are equal; this is physically equivalent to assuming that the electron-hole recombination time is much shorter than the phonon period. We note that those calculations were for substantially larger electron-hole densities than in the present case, so that electron-hole recombination times may indeed have been much shorter. We will briefly discuss the results of calculations using $\mu_{e^-} = \mu_{h^+}$ for the present system.

The stable form of tellurium at low pressure is α-Te, in which twofold coordinated tellurium atoms form infinite helical chains parallel to the **c** axis of the trigonal $P3_121$-D_3^4 structure [11]. The three atoms per unit cell are at $(x0\frac{1}{3}, 0x\frac{2}{3}, \overline{xx}0)$ and form a single, complete turn of a helical chain. Each helix is surrounded by six equidistant helices and each atom has four second-nearest neighbors in these adjacent helices. The atomic position free parameter x is equal to the ratio of the radius of each helix to the interhelical distance.

The experimentally determined equilibrium value of x is $x_{\mathrm{equil}} = 0.2633 \pm 0.0005$ and the room-temperature lattice constants are $a = 4.4561$ Å and $c = 5.9271$ Å. At these values, the bond length is 2.834 ± 0.002 Å, the bond angle is $103.2° \pm 0.1°$, and the second-nearest-neighbor distance is 3.494 Å [11].

The motion of atoms in the A_1 phonon mode corresponds to a variation of the helical radius x, maintaining the symmetry of the crystal. We note that the equilibrium value of x is not determined by symmetry, and so may be expected to change in the photoexcited material, allowing DECP excitation of this mode.

At the special value, $x = 1/3$, the nearest-neighbor and second-nearest-neighbor distances become equal, the atomic coordination number increases to six, the helical chain structure is destroyed, and the structure can be classified as rhombohedral, with space group $R\overline{3}m$-D_{3d}^5 and one atom per unit cell. The high-pressure γ-Te form of tellurium, which is stable above $\sim$70 kbar, has this structure [11]. The α-Te structure may be viewed as a Peierls distortion of the γ-Te structure, as we shall see below.

We have calculated structural total energies as a function of the A_1 symmetry phonon displacement x and determined the vibrational frequency using the "frozen phonon" method [12]. Total energy calculations were performed using the plane-wave pseudopotential method and the local density approximation (LDA) to exchange and correlation [13–15]. Plane waves up to energy cutoffs of 16 and 49 Ryd were used in the expansion of the wave functions and the charge density, respectively. Self-consistent potentials, total energies, and electronic densities of states were calculated using a regular $10 \times 10 \times 10$ grid in the full Brillouin zone (124 k points in the irreducible zone), with the following constraints on the occupation of states: States in the valence bands (i.e., bands 1–9) at each k point were weighted by the Fermi-Dirac distribution with a temperature T and a chemical potential μ_{h^+}. The value of μ_{h^+} is chosen to ensure the correct number of holes in the valence bands, corresponding to the appropriate electron-hole density. Similarly, the states in the conduction bands (i.e., bands 10 and above) were filled according to the Fermi-Dirac distribution with temperature T and chemical potential μ_{e^-}.

We note that the LDA performs less well in the prediction of ground state structural and vibrational properties for Te than for systems such as silicon and diamond [12], principally in that it underestimates the interchain repulsive forces [16,17], leading to an interchain distance 3.8% smaller than experiment. For the results reported below, we have used the experimentally determined room-temperature lattice constants. However, we find that the results are not significantly different if we use the LDA theoretical equilibrium lattice parameters: The phonon frequency for zero density of photoexcited carriers is 15% smaller and the magnitude of the derivative of the phonon frequency with respect to excited carrier density is 20% larger.

We use the zero-temperature LDA exchange-correlation potential to calculate the effects of exchange and correlation in the photoexcited system. The motivation for this approximation in the present context is the same as in using the zero-temperature LDA to calculate exchange and correlation in finite-temperature calculations [18] or in constrained density-functional theory (DFT) calculations [19]. In general, the use of LDA band energies for excited states is complicated by the fact that the true (quasiparticle) excitation energies are not equal to the DFT eigenvalues. However, in this system the LDA gap (0.26 eV) is not too much different from the experimental band gap (0.33 eV [20]), and the band dispersions within the LDA conduction and valence bands are very similar to the experimentally determined dispersions [21]. Moreover, although the details of the band dispersions and band gaps change substantially when the experimental lattice constants are replaced by their theoretical equilibrium values [16], the phonon frequencies do not change drastically (see above). Thus, the approximation of using the LDA excited bands to calculate the total energy of the photoexcited system is reasonably accurate in the present context.

We have calculated the A_1 phonon frequency in the photoexcited system for a range of electron temperatures up to $k_BT = 0.2$ eV. We find that the electron temperature has a negligible effect on the phonon frequency. This insensitivity to temperature is qualitatively important, implying that the results we have obtained are not strongly

dependent on the assumption of a thermal distribution of carriers or on the details of the band dispersions within the conduction and valence bands; the dominant effect on the phonon frequency is due simply to the number of carriers excited to the conduction (antibonding) states, not their precise distribution within those states. In particular, possible slow relaxation of carriers (e.g., between different conduction band minima) should not strongly affect the phonon frequencies.

Figure 1 shows the structural energy as a function of x for excited carrier densities ranging from 0% to 1.25% of the valence electron density. The ground state equilibrium value of x is found to be 0.2686, approximately 2% larger than the experimental value of 0.2633. The frequency of oscillation about this minimum was calculated as 3.24 THz, 10% smaller than the value obtained in conventional Raman scattering of 3.6 THz. This accuracy is typical of LDA calculations for such materials [16,17,22].

The maximum at $x = 1/3$ in Fig. 1 is due to a high degeneracy of states near the Fermi level for this high symmetry structure. This degeneracy is lifted for $x \neq 1/3$, lowering the energy of the occupied electronic states and the structural energy, in a striking example of a Peierls (or static Jahn-Teller) distortion. The high sensitivity of the A_1 phonon mode to photoexcitation is a direct consequence of this mechanism for stabilization of the α-Te structure: Occupation of states just above the Fermi level in the photoexcited material greatly reduces the stabilizing effect of the Peierls mechanism.

Within the DECP mechanism, the initial amplitude of phonon motion is equal to $|x_{\mathrm{equil}} - x^0_{\mathrm{equil}}|$, where x_{equil} is the position of the energy minimum for the photoexcited system and x^0_{equil} is the minimum for the unexcited system. The energy vs x curves are significantly anharmonic and so the period of motion changes with amplitude.

Figure 2(a) shows the linear increase of the equilibrium bond length with carrier excitation density, clearly demonstrating the weakening of the bonds and the displaced equilibrium that results from electrons occupying antibonding states. Figure 2(b) shows the dependence of frequency on excitation density for the initial DECP amplitude and for small amplitude motion. For all carrier densities, the anharmonic terms tend to lower the phonon frequency. Thus, even in the absence of carrier diffusion, the DECP phonon period will decrease on successive cycles of the motion, as damping reduces the amplitude. However, the initial amplitude of DECP motion is large enough to make this effect appreciable only for photoexcited carrier densities greater than approximately 1% of the valence electron density.

In comparison with the above results, if we assume that the electron-hole recombination time is much smaller than the phonon period (i.e., that $\mu_{h^+} = \mu_{e^-}$ and that electron-hole excitation is caused by maintaining the electronic system at a very high temperature [10]), we find qualitatively different behavior of the phonon frequency and the equilibrium helical radius: As the temperature is increased, the phonon period increases and the helical radius decreases. The reason for this [21] is that the splitting between valence and conduction bands is strongly affected by the phonon coordinate x, leading to a rapid increase in the

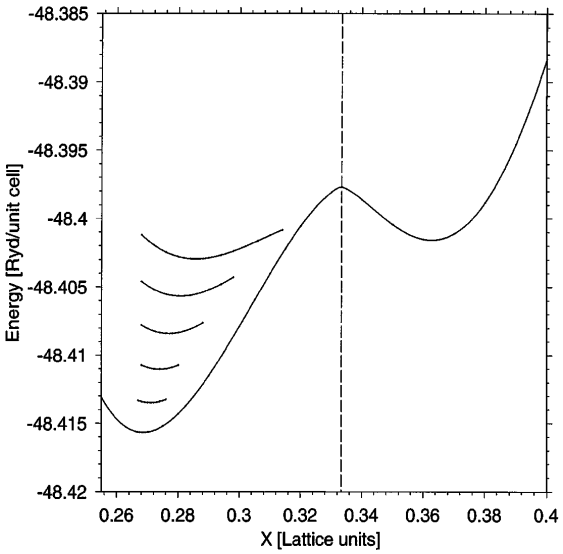


FIG. 1. Total energy per unit cell as a function of phonon coordinate x for photoexcited electron densities of 0% (lowermost curve), 0.25%, 0.5%, 0.75%, 1.0%, and 1.25% (uppermost curve) of the valence electron density. The dashed line indicates the value of $x = 1/3$ for the high symmetry γ-Te structure. The curves are cubic spline fits through the calculated points.

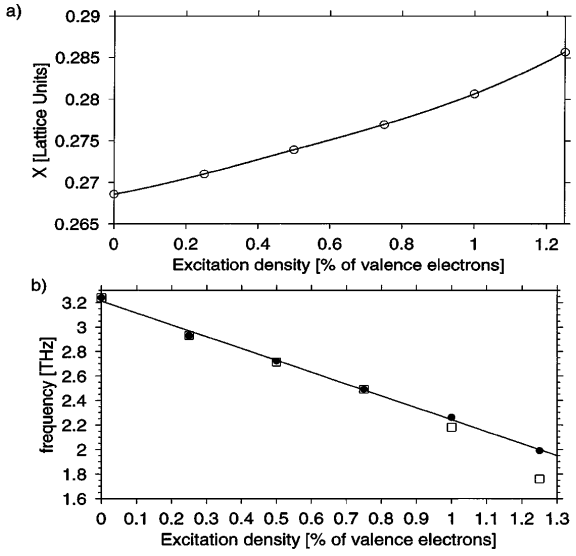


FIG. 2. (a) Equilibrium bond length and (b) A_1 phonon frequency versus photoexcited carrier density. The curve in (a) is a cubic spline fit through the calculated points. The frequency in (b) is shown for the initial DECP amplitude motion (open squares) and for the final, small amplitude motion (solid dots). The slope of the linear fit to the small amplitude frequencies in (b) corresponds to a frequency shift of -0.97 THz for 1% of the valence electrons excited into the conduction bands.

electron-hole density as x increases while keeping the temperature constant.

In light of these calculations, we can offer new insight into the recent pump-probe measurements of the A_1 phonon in tellurium. Hunsche *et al.* [3] measured the phonon frequency for pump fluences up to 12.5 mJ/cm^2 and found a systematic decrease in frequency from 3.6 THz for the lowest pump fluences to 2.95 THz for the largest. This reduction in phonon frequency with increasing pump fluence is consistent with the linear decrease in phonon frequency with photoexcited carrier density found in the calculations above. For example, for a pump fluence of 2.4 mJ/cm^2, Hunsche *et al.* estimate an initial surface carrier density of 1.1×10^{21} cm^{-3}, or 0.7% of the valence electron density. Carrier diffusion at normal diffusion rates ($D = 40$ cm^2/s) reduces the surface carrier density by a factor of 0.52 in the first phonon period. For this pump fluence, the A_1 phonon frequency, as measured by the probe reflectivity oscillations, is 0.1–0.2 THz lower than its frequency in the unexcited system (see Fig. 3 of Ref. [3]). Using the calculated phonon frequency as a function of carrier density [Fig. 2(b)], this frequency change would imply a surface carrier density of 0.1%–0.2% of the valence electron density, approximately 50% smaller than the assumptions of linear absorption and normal carrier diffusion rates would imply. Given the uncertainties in the experimental measurements and the theoretical calculations, this agreement is quite satisfactory but may suggest that either (a) electron-hole pair production is somewhat less efficient than linear absorption would imply or (b) the carrier diffusion rate is somewhat higher than normal at these highly excited carrier densities. Moreover, the decrease in the period for successive oscillations at very high pump fluence, where the phonon frequency is 0.3–0.6 THz lower than its value in the unexcited system (Fig. 3 of Ref. [3]), is too large to be due to anharmonicity of the phonon motion, as shown in Fig. 2(b) for carrier densities of approximately 0.6% of the valence electron density. This supports the hypothesis in Ref. [3] that this is due to carrier diffusion, leading to a reduction of the surface carrier density.

In conclusion, we have calculated, using *ab initio* band structure methods, the dependence of the A_1 phonon frequency in tellurium on photoexcited carrier density, assuming fast thermalization of the carrier distribution and slow electron-hole recombination. We have also determined the initial amplitude of phonon motion, and the resulting anharmonic corrections to the period, within the DECP mechanism for the photoexcited system. The calculations shed new light on the interpretation of existing pump-probe experiments and open the possibility of using real-time measurements of the A_1 phonon period to monitor the evolution of carrier densities in photoexcited tellurium on a subpicosecond time scale. Similar calculations are feasible for many other materials.

This work has been supported by Forbairt Contract No. SC/96/742.

[1] Jagdeep Shah, *Ultrafast Spectroscopy of Semiconductors and Semiconductor Nanostructures*, Springer Series in Solid State Sciences Vol. 115 (Springer, Berlin, 1996).
[2] R. Merlin, Solid State Commun. **102**, 207 (1997).
[3] S. Hunsche, K. Wienecke, T. Dekorsky, and H. Kurz, Phys. Rev. Lett. **75**, 1815 (1995).
[4] H. J. Zeiger, J. Vidal, T. K. Cheng, E. P. Ippen, G. Dresselhaus, and M. S. Dresselhaus, Phys. Rev. B **45**, 769 (1992).
[5] W. Z. Lin, J. G. Fujimoto, E. P. Ippen, and R. A. Logan, Appl. Phys. Lett. **50**, 124 (1987); **51**, 161 (1987); W. Z. Lin, R. W. Schoelein, J. G. Fujimoto, and E. P. Ippen, IEEE J. Quantum Electron. **24**, 267 (1988).
[6] M. Rasolt, Phys. Rev. B **33**, 1166 (1986).
[7] See, for example, C. Kittel and H. Kroemer, *Thermal Physics* (Freeman, San Francisco, 1980), Chap. 15.
[8] R. Biswas and V. Ambegaokar, Phys. Rev. B **26**, 1980 (1982); Phys. Rev. Lett. **50**, 285 (1983).
[9] P. Stampfli and K. H. Bennemann, Phys. Rev. B **42**, 7163 (1990); **46**, 10 686 (1992); **49**, 7299 (1994).
[10] P. L. Silvestrelli, A. Alavi, M. Parrinello, and D. Frenkel, Phys. Rev. Lett. **77**, 3149 (1996); Phys. Rev. B **56**, 3806 (1997).
[11] Jerry Donohue, *The Structures of the Elements* (Wiley Interscience, New York, 1974).
[12] W. E. Pickett, Comput. Phys. Rep. **9**, 115 (1989).
[13] J. Ihm, A. Zunger, and M. L. Cohen, J. Phys. C **4**, 4409 (1979).
[14] D. R. Hamann, M. Schlüter, and C. Chiang, Phys. Rev. Lett. **43**, 1494 (1979).
[15] J. P. Perdew and A. Zunger, Phys. Rev. B **23**, 5048 (1981).
[16] F. Kirchoff, N. Binggeli, G. Galli, and S. Massida, Phys. Rev. B **50**, 9063 (1994), and references within.
[17] G. Kresse, J. Furthmüller, and J. Hafner, Phys. Rev. B **50**, 13 181 (1994).
[18] A. Alavi, J. Kohanoff, M. Parrinello, and D. Frenkel, Phys. Rev. Lett. **73**, 2599 (1994).
[19] A. K. McMahan, R. M. Martin, and S. Satpathy, Phys. Rev. B **38**, 6650 (1988).
[20] V. B. Anzin, M. I. Eremets, Yu. V. Kosichkin, A. I. Nadezhdinskii, and A. M. Shirokov, Phys. Status Solidi A **42**, 385 (1977).
[21] P. Tangney, M.Sc. thesis, University College, Cork, 1998 (unpublished); P. Tangney and S. Fahy (to be published).
[22] F. Mauri, O. Zakharov, S. de Gironcoli, S. G. Louie, and M. L. Cohen, Phys. Rev. Lett. **77**, 1151 (1996).